Many-Nucleon Transfer Reactions of the Type (d,Li^7), (d,Be^7), and (d,Be^9) at 15 MeV*

L. J. Denes† and W. W. Daehnick
University of Pittsburgh, Pittsburgh, Pennsylvania
(Received 21 September 1966)

Differential cross sections have been measured for (d,Li^7) and $[d,Li^{7*}(0.478)]$ reactions from C^{13}, O^{17}, O^{18}, and F^{19} as well as for $F^{19}(d,Be^7)$, $F^{19}[d,Be^{7*}(0.432)]$, $F^{19}(d,Be^9)C^{12}$, and $F^{19}(d,Be^9)C^{12*}(4.43)$, utilizing simultaneous time-of-flight and energy analysis. All 12 angular distributions for these many-nucleon transfer reactions were obtained at incident deuteron energies near 15 MeV, and show forward peaking and noticeable, diffraction-like structure as well as large total cross sections ($0.1<\sigma_{tot}<1.8$ mb). Hence most (d,Li^7) cross sections reported here are comparable in magnitude to those of (d,Li^6) reactions from corresponding targets. An interpretation of these many-nucleon transfers in terms of a simple direct-reaction model is attempted. Distorted-wave Born-approximation (DWBA) calculations were made, analogous to earlier calculations for (d,Li^6) angular distributions on similar targets. DWBA curves with a damped diffraction structure are obtained easily, since for 5-nucleon transfers, the angular distribution usually has contributions from two different l transfers. Our DWBA calculations for these reactions yield the correct order of magnitude for the absolute total cross sections, and qualitative agreement in the angular distributions. Tentative spectroscopic coefficients are extracted from the comparison of experiment and calculations.

A. INTRODUCTION

FOR intermediate deuteron energies, direct-reaction mechanisms have been successfully used to interpret one-, two-, and even three-particle transfers. Nevertheless, it is not certain that the transfer of larger groups of nucleons will be amenable to the same simple treatment. For example, it is conceivable that the rearrangement of a 15-nucleon system, such as $C^{13}+d$ into Be^8+Li^7, could be viewed as the decay of a highly excited N^{15} compound state by Li^7 emission, or as some form of induced fission. It appears at this time that 5-nucleon transfer reactions have strong compound features at low c.m. energies,[1] but depending on target and reaction energy, direct-reaction contributions may become important at several MeV (c.m.).[2] For deuterons of 12 MeV or higher, (d,Li^7) reactions consistently show features, such as diffraction-type angular distributions, normally associated with direct reactions.[3,4]

This study of 5-nucleon transfers primarily presents experimental and theoretical cross sections for $C^{13}(d,Li^7)Be^8$, $O^{17}(d,Li^7)C^{12}$, $O^{18}(d,Li^7)C^{13}$, $F^{19}(d,Li^7)N^{14}$, and $F^{19}(d,Be^7)C^{14}$. Data were taken at measured deuteron energies near 15 MeV. The exact energies differed from one angular distribution to another by up to a few hundred keV, as shown later. No drastic energy dependence was observed in these runs. We report a DWBA analysis in terms of a very simple direct cluster transfer model,[5] which should be viewed as a first attempt to explain the general features and the magnitude of the cross sections in these reactions. Our direct-reaction interpretation is supported by consistent forward peaking of the experimental angular distributions and the large reaction cross sections observed, but no claim is made that other reaction mechanisms may be completely neglected or that our simple DWBA model is sufficiently complete, even in the framework of direct-reaction theory. The primary motivation for the performance of these DWBA calculations was their great potential use in the spectroscopy of light elements and the relative ease with which they could be performed.

B. EXPERIMENTAL PROCEDURE

The bombardment of very thin targets (16–100 $\mu g/cm^2$) containing C^{13}, O^{17}, O^{18}, or F^{19} yields a variety of fast ions with comparable and fairly large cross sections. In a previous paper[6] we have given a detailed description of the experimental methods used to detect and identify Li^6 ions. The experimental detection apparatus which was developed for the unique identification of Li ions[6,7] from (d,Li^6) reactions also provides good separation for mass-7 and -9 particles. This report concentrates on the heavier ions such as Li^7, Be^7, and Be^9 which were produced and detected along with the Li^6 particles. In all cases for which cross sections are presented, simultaneous energy and time-of-flight

* Work done at the Sarah Mellon Scaife Radiation Laboratory, and supported in part by the National Science Foundation.
† Present address: United Aircraft Research Laboratories, East Hartford, Connecticut.
[1] J. M. Blair and R. H. Hobbie, Phys. Rev. **128**, 2282 (1962); G. C. Morrison, *ibid.* **121**, 182 (1961).
[2] D. W. Heikkinen, Phys. Rev. **141**, 1007 (1966); R. R. Carlson and R. L. McGrath, Phys. Rev. Letters **15**, 173 (1965); R. L. McGrath, Phys. Rev. **145**, 802 (1966).
[3] D. Dehnhard, D. S. Gemmel, and Z. Vager, Bull. Am. Phys. Soc. **10**, 462 (1965); R. S. Bender and E. Newman, *ibid.* **10**, 602 (1965).
[4] L. J. Denes and W. W. Daehnick, Bull. Am. Phys. Soc. **10**, 120 (1965); W. W. Daehnick and L. J. Denes, *ibid.* **11**, 30 (1966).
[5] R. M. Drisko, G. R. Satchler, and H. R. Bassel, in *Proceedings of the Third Conference on Reactions between Complex Nuclei, Asilomar, 1963*, edited by A. Ghiorso, R. M. Diamond, and H. E. Conzett (University of California Press, Berkeley, California, 1963).
[6] W. W. Daehnick and L. J. Denes, Phys. Rev. **136**, B1325 (1964).
[7] L. J. Denes, W. W. Daehnick, and R. M. Drisko, Phys. Rev. **148**, 1097 (1966).

analyses were sufficient to identify and separate groups resulting from different ions or final states.

A deuteron beam of 14.5 to 15 MeV from the Pittsburgh fixed-energy cyclotron was magnetically analyzed, and typically showed about 1° angular divergence and an energy spread of less than 80 keV. The inherent rf structure of the analyzed cyclotron beam led to deuteron beam pulses of less than 2 nsec in duration, which arrived at intervals of about 88 nsec. The timing signal T_0 for the time-of-flight circuit was derived from a plastic scintillation counter detecting elastically scattered deuterons. A 200-μ-thick gold surface-barrier detector was used to detect and stop all heavy reaction products, typically after a 1 m flight from the target. This detector provided an energy pulse to one side of a two-dimensional multichannel analyzer, and simultaneously, a second timing signal T_1. A pulse proportional to the time difference between the occurrence of the deuteron beam signal T_0 and the time T_1, $P\sim T_1-T_0$, then was fed to the second input of the analyzer. As simultaneous information of energy and velocity determines the ion mass, the additional knowledge of the reaction Q-values uniquely identified the isotopes detected for all reactions under discussion.

In addition to the reactions mentioned above, we had hoped to identify and measure the (d,Li^8) reaction from O^{18}; however, the current time-of-flight apparatus was not capable of separating the very low energy mass-eight particles from the background. The $O^{18}(d,\mathrm{Li}^8)C^{12}$ Q value is -8.61 MeV, hence at $E_d\simeq 15$ MeV the Li^8 ions are emitted below the Coulomb barrier (barrier penetrability $\simeq 0.3$), and not only the Li^8 energy but also the expected cross section is small. The search for Li^{8+++} ions ($Z^2/A=1.125$) by magnetic analysis was also unsatisfactory because of an ambiguity created by a strong group of C^{14++++} recoils ($Z^2/A=1.143$) which at forward angles were also close to the Li^8 ions in kinetic energy. The ambiguity finally was removed by the simultaneous measurement of time-of-flight, magnetic rigidity, and energy of the reaction products. As the particle trajectory through our analyzing magnet was 250 cm long, the time-of-flight measurement gave very good mass separation. A typical energy spectrum (for a given magnetic rigidity and summed over the time-of-flight dimension) is shown in Fig. 1. All mass groups were widely separated in the time-of-flight dimension and had flight times corresponding to the indicated mass identification. The arrows indicate the predicted energies of the ion groups. It is of interest to note that the heavy recoils listed as $(\mathrm{Mass}\ 15)^{++++}$ and C^{14++++} do not quite give the pulse height in the Au surface-barrier solid-state detector which is expected from their known energy (Z^2/A ratio).[8] With this improved particle identification system, a search at the appropriate energy regions did not yield any significant particle group which could be identified as Li^{8+++} ions from the $O^{18}(d,\mathrm{Li}^8)C^{12}$ reaction.

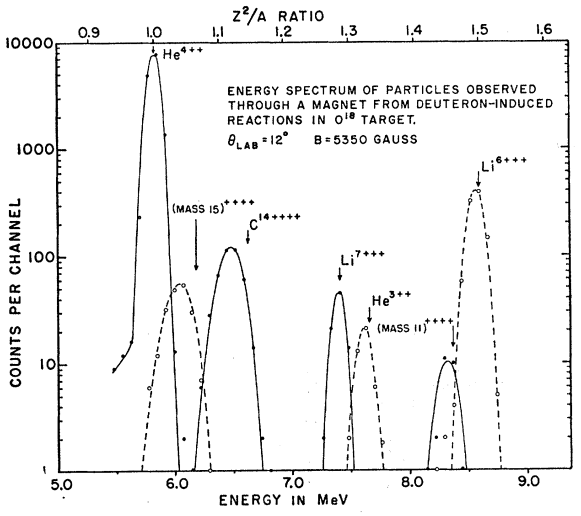

FIG. 1. Spectrum from a solid-state counter at the focal plane of an analyzing magnet for a fixed field B. The energy of the detected charged particle is proportional to Z^2/A (top scale). The mass identification was verified by additional time-of-flight analysis.

C. EXPERIMENTAL RESULTS

Examples of energy spectra for the heavy reaction products, which were separated according to mass by time-of-flight analysis, are presented in Fig. 2. The general characteristics of the individual spectra are similar to the $M=6$ spectra from corresponding targets as shown in Refs. 6, 7; but, in contrast to the Li^6 spectra, the particle-stable first excited states of both the Li^7 and Be^7 ions are seen. All prominent groups have been identified as transitions leaving the product nuclei either in their ground states or lower excited states. Mass-7 or -9 ions from C^{12} and O^{16} contaminants are not observed since these reactions are prohibited by their large negative Q values. The $C^{13}(d,\mathrm{Li}^7)\mathrm{Be}^8$ reaction [Fig. 2(a)] has a spectrum similar to the $C^{12}(d,Li^6)\mathrm{Be}^8$ reaction (see Ref. 6) although the $M=7$ spectrum shown is more complicated. The C^{13} target consisted of a Ni backing with carbon deposits on both surfaces[7]; consequently Li^7 ions from the far surface are degraded in energy to about 1 MeV below corresponding Li^7 ions from the near surface, and thus create a "ghost" spectrum. An additional complication arises from excited (0.478 MeV) Li^7 ions produced by the $(C^{13}+d)$ reaction.

The F^{19} target was made just thin enough so that the emitted Li^7, $\mathrm{Li}^{7*}(0.478)$, Be^7, and $\mathrm{Be}^{7*}(0.432)$ ions could be separated using their predicted energy positions and expected widths [Fig. 2(d)]. The $M=9$ spectrum [Fig. 2(e)], on the other hand, contains only nonexcited Be^9 ions from the $F^{19}(d,\mathrm{Be}^9)$ reactions, leaving C^{12} in

[8] R. C. Axtmann and D. Kedem, Nucl. Instr. Methods 32, 70 (1965); P. G. Bizzeti, A. M. Bizzeti Sona, G. DiCapariacco, and M. Mando, *ibid.* 34, 261 (1965); L. Van de Zwan, C. D. Porterfield, and R. C. Ritter, *ibid.* 24, 329 (1963).

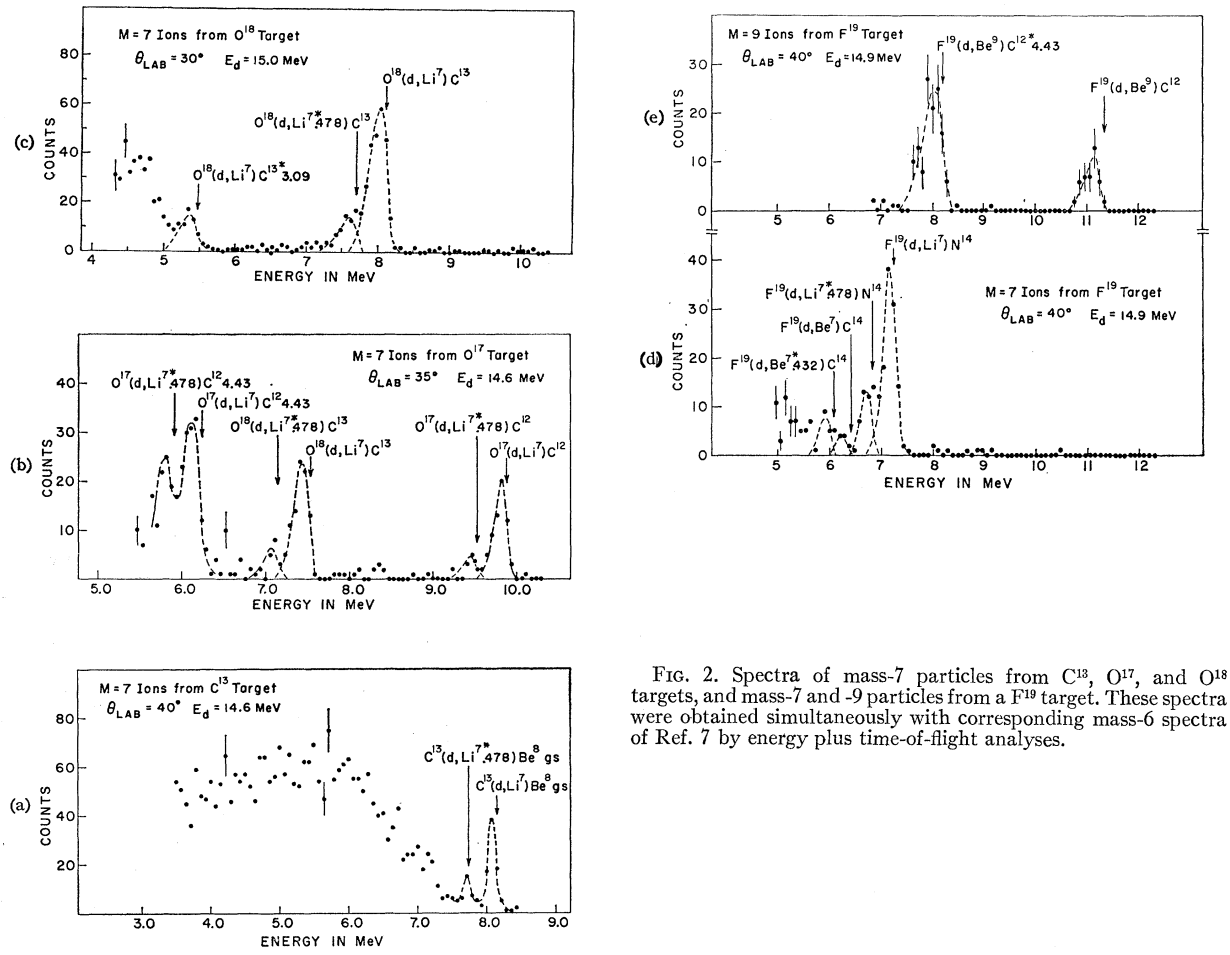

FIG. 2. Spectra of mass-7 particles from C^{13}, O^{17}, and O^{18} targets, and mass-7 and -9 particles from a F^{19} target. These spectra were obtained simultaneously with corresponding mass-6 spectra of Ref. 7 by energy plus time-of-flight analyses.

the ground state or the 4.43-MeV state. From the spectra in Figs. 2(b), 2(e), it is quite apparent that, although energetically disfavored by over 4 MeV, the transition to the 4.43-MeV state in C^{12} is much stronger than the ground-state transition in both the $O^{17}(d,Li^7)$ and the $F^{19}(d,Be^9)$ reactions.

The center-of-mass angular distributions for (d,Li^7) and $(d,Li^{7*}$ 0.478) reactions from C^{13}, O^{17}, O^{18}, and F^{19} are shown in Fig. 3, while (d,Be^7), $(d,Be^{7*}$ 0.432), $(d,Be^9)C^{12}$, and $(d,Be^9)C^{12*}$ (4.43) reactions from F^{19} are shown in Fig. 4. In general, these angular distributions are not markedly different in character from those for (d,Li^6) reactions (see Ref. 7), although the reactions are inherently more complicated. All angular distributions are forward-peaked and have surprisingly large forward-angle cross sections ($\sim$100 μb/sr). However, there is less diffractive structure than in the (d,Li^6) angular distributions. Such lack of diffractiveness for these mass-7 reaction products is not inconsistent with the DWBA picture. The cluster pickup model[7] allows two values of l transfer for each reaction from these targets with the exception of the reaction $F^{19}(d,Be^9)$-C^{12}g.s. In general an incoherent addition of two contributions to the cross section from different l transfers will lead to less distinctive and smoother angular distributions.

Total cross sections for the (d,Li^7), (d,Be^7), and (d,Be^9) reactions were estimated by using the DWBA curves shown in Figs. 3 and 4 for extrapolation to 180°, and are listed in Table I. Also listed, for the sake of comparison, are estimated total cross sections for (d,Li^6) reactions[7] from corresponding targets. The (d,Li^7) and (d,Li^{7*}) cross sections are quite comparable to those of (d,Li^6) reactions from the same targets. The largest discrepancy occurs in F^{19}, where the (d,Li^7) cross sections are significantly smaller than that for (d,Li^6). This is not too surprising since the Q values for these (d,Li^7) reactions are more negative by about 4 MeV than for the (d,Li^6) reaction, which leads to a decrease in the barrier penetrability factor. Similarly in the (d,Be^7) reactions, where the barrier penetrability has decreased even further, the total cross sections have decreased in like manner. The $F^{19}(d,Be^9)C^{12}$ data show that even seven nucleons can be transferred with relatively large cross sections in the deuteron bombardment on light nuclei. The $F^{19}(d,Be^9)$ reaction leading to

the C^{12*} 4.43 state is four times stronger and comparable to the $F^{19}(d,Li^7)$ reaction.

The $O^{17}(d,Li^7)$ and $O^{17}(d,Li^{7*})$ reactions were measured at 14.6, 14.8, and 14.9 MeV and the $F^{19}(d,Be^9)C^{12}$ reaction was measured[6] at 14.5 and 14.9 MeV, but the statistics were too poor to assess the magnitude of the energy-dependent effects. The $O^{17}(d,Li^7)$ and $O^{17}(d,Li^{7*})$ data given represent a weighted average of the three runs.

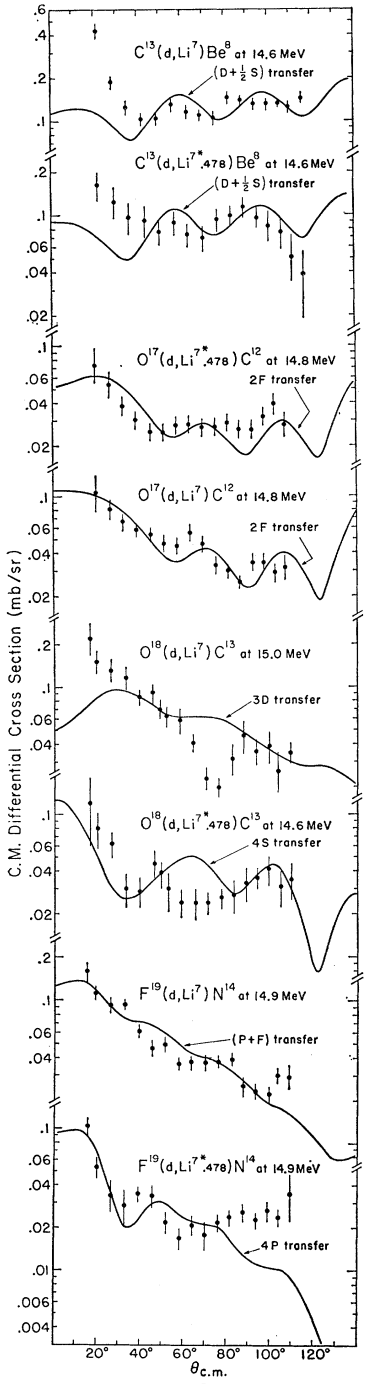

FIG. 3. Experimental and theoretical angular distributions in the center-of-mass system for (d,Li^7) and (d,Li^{7*}) reactions in light nuclei. The error bars contain all random experimental errors. The solid curves are DWBA predictions. Two values of l transfer may generally contribute in these reactions.

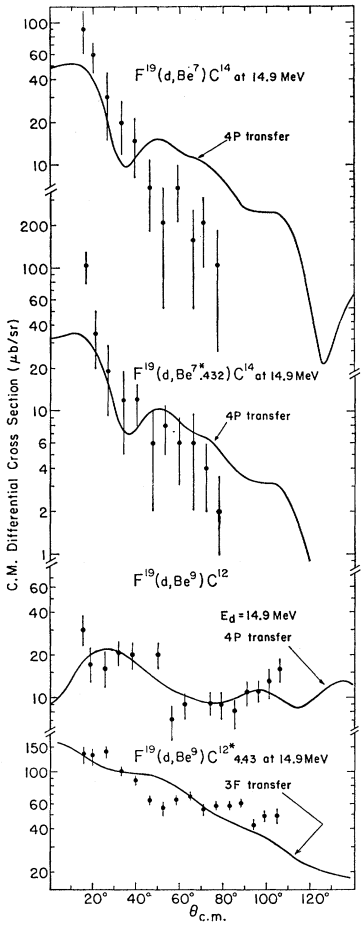

FIG. 4. Experimental and theoretical angular distributions in the center-of-mass system for (d,Be^7), (d,Be^{7*}), and (d,Be^9) reactions from F^{19}. The error bars contain all random experimental errors. The curves are DWBA predictions.

Experimental Errors

The largest experimental random errors generally are due to statistics. Other random errors result from the subtraction of background and from imperfect separation of nearby groups in the three-dimensional energy-velocity-counts space. All these random errors were estimated and added as the sum of their squares, and are shown in Figs. 3 and 4 by errors bars.

Systematic errors are not shown in the figures. They are due to an uncertainty in the zero angle of $\Delta\theta_0=\pm1°$ and uncertainties in the target thickness. For the very thin targets, effects of nonuniformity may be appreciable and comparable to the 10% error in the determination of the average target thickness. Errors in geometry and beam collection are small by comparison, and we assign an over-all uncertainty of $\pm20\%$ to our absolute-cross-section scale.

This scale error of 20% must be kept in mind when comparing the yield of different reactions from *different* targets. However, no such uncertainty applies to the comparisons of, for instance, $O^{18}(d,Li^6)$ (in Ref. 7) to $O^{18}(d,Li^7)$ in this paper, as Li^7 and Li^6 ions from a given target were detected simultaneously.

TABLE I. Total cross sections and spectroscopic coefficients for various many-nucleon transfer reactions.

Reaction	Exper. total cross section (mb)	Approx. barrier penetrability	l transfer	Rel. spectroscopic coeff.
$C^{13}(d,Li^7)Be^8$	1.65	0.95	0	0.10[a]
			2	0.21
$C^{13}(d,Li^{7*})Be^8$	1.18	0.95	0	0.13[a]
			2	0.27
$O^{17}(d,Li^7)C^{12}$	0.53	0.90	3	0.46
$O^{17}(d,Li^{7*})C^{12}$	0.39	0.90	3	0.70
$O^{18}(d,Li^7)C^{13}$	0.62	0.80	2	0.38[a]
$O^{18}(d,Li^{7*})C^{13}$	0.38	0.80	0	0.56[a]
$F^{19}(d,Li^7)N^{14}$	0.48	0.60	1	0.53
			3	0.53
$F^{19}(d,Li^{7*})N^{14}$	0.27	0.60	1	1.3
$F^{19}(d,Be^7)C^{14}$	0.10	0.25	1	0.60
$F^{19}(d,Be^{7*})C^{14}$	0.09	0.15	1	1.5
$F^{19}(d,Be^9)C^{12}$	0.15	0.95	1	0.13
$F^{19}(d,Be^9)C^{12*}(4.43)$	0.62	0.75	3	0.62
$C^{12}(d,Li^6)Be^8$	4.2	0.90	0	0.60
$C^{13}(d,Li^6)Be^9$	2.0	0.50	2	1.2
$O^{16}(d,Li^6)C^{12}$	2.9	0.80	0	3.0
$O^{17}(d,Li^6)C^{13}$	0.65	0.85	3	0.30
$O^{18}(d,Li^6)C^{14}$	0.60	0.85	0	0.20
$F^{19}(d,Li^6)N^{15}$	1.4	0.90	1	0.30[a]

[a] Poor fit.

D. DWBA CALCULATIONS FOR (d,Li^7), (d,Be^7), AND (d,Be^9) REACTIONS

All cross sections were calculated as a direct-reaction one-step pickup using code JULIE.[7] The (d,Li^7) reaction was assumed to be of the type (B+He^5)(d,d+He^5)B, and the same prescriptions were used as for the previous (d,Li^6) DWBA calculations.[7] The goal of this analysis was to obtain a systematic set of DWBA calculations for the (d,Li^7) reactions, consistent with the (d,Li^6) calculations, so that the uncertainties and biases in the calculations are nearly identical, and spectroscopic comparisons may be made. The same best-fit deuteron scattering parameters were used for the incident deuteron channel, and the same optical parameters for Li^7 were used for the exit channels.[7] Of course, the distorted waves generated by these potentials must differ somewhat on account of mass, charge, and energy differences. The form factor is obtained by a procedure analogous to that used for the "quasi-alpha-particle" transfer.[7] Hence, the "wave function of the transferred cluster" is restricted to orbital angular momenta l needed for the transition under consideration, and to a corresponding main quantum number N derived from the simple shell-model (independent-particle-model) wave functions of the constituent nucleons. For a five-particle cluster, the lowest internal-energy quantum is one, and this value was always used. Both $J^\pi=\frac{1}{2}^-$ and $\frac{3}{2}^-$ are allowed in a quasi-He^5 cluster, and, as the deuteron spin is 1, two l values are normally allowed in quasi-He^5 transfers to known final states.

A Saxon well of radius 2.2 $A^{1/3}$ F and diffusivity 0.8 F was used to generate the "cluster wave function." The form-factor potentials for more complex clusters (five or seven nucleons) should be expected to differ somewhat from those for alpha clusters, but in the absence of guiding scattering potentials we have retained the well geometry used previously for (d,Li^6) calculations. Again, we have not used radial cutoffs in the calculations which are compared with experiment.

The absolute normalization for these calculations has been estimated in the same manner as for the (d,Li^6) reactions.[7] The normalization factor A contains a quantity a_0^2, the probability that the Li (or Be) wave functions can be written as deuteron plus transferred cluster, or $\psi_{\text{cluster}}\phi_d$. In the Li^6 case, one has good reasons to believe that $a_0^2\simeq 1$. For Li^7, Be^7, and Be^9, a_0^2 is not known, and one may allow $0.1<a_0^2<0.8$. The spectroscopic coefficients in Table I are based on the assumptions $a_0^2(\text{Li}^6)=1$ and $a_0^2(\text{Li}^7)=a_0^2(\text{Be}^7)=0.4$. The normalization A for (d,Be^9) could not be estimated with any confidence and arbitrarily was set equal to that for (d,Li^6). With such absolute normalizations, the DWBA predictions are of the same order of magnitude as the experimentally observed cross sections, apart from the "spectroscopic factors for effective He^5 clustering." It must be mentioned, however, that the magnitude of the DWBA predictions for reactions with *low* (≤ 0.5) barrier penetrability factors is strongly dependent on the size of the form-factor well, and "reasonable" changes in r_0 or diffusivity a may change the extracted spectroscopic coefficients by factors of 2 or 3.

E. DISCUSSION

Our experimental angular distributions are compared with DWBA predictions in Figs. 3 and 4. We have neglected spin-orbit interactions, and hence treat contributions to the cross sections from different allowed l values as incoherent, so that the predicted cross sections for given l transfers may be summed. The adjusted sum of two l-transfer predictions is shown only where the summation will lead to agreement which is clearly superior to a single l-value prediction. It can easily be seen that the addition of predictions for two different l values will remove much of the diffractive nature of the individual angular distributions. In many cases we observe good qualitative agreement between data and the DWBA calculations, but there are also cases of obvious disagreement for very small and very large angles. Disagreement for $\theta>70°$ often has been found also in much simpler stripping reactions, and may partly be due to the neglect of the particle spins in the calculations. This difficulty is not easily remedied if both reaction particles have spins larger than $\frac{1}{2}$. Disagreement at small angles, where simple DWBA should be best, may be attributable to the crude approximation for the unknown Li^7 waves It is gratifying that for the two examples where both ingoing (d) and outgoing (Li^7) waves are realistic, i.e., in

the $O^{17}(d,Li^7)C^{12}$ and $O^{17}(d,Li^{7*})C^{12}$ reactions, quite good agreement at all angles is found for a single l-transfer ($2F$) assignment (see Fig. 3).

Actually, the calculations give a fair semblance to most data with the exception of the $O^{18}(d,Li^7)C^{13}$, $O^{18}(d,Li^{7*})C^{13}$, and $F^{19}(d,Be^9)C^{12*}$ angular distributions. Our Li^7 parameters are probably not useful for the generations of Be^9 waves, and detailed agreement for $F^{19}(d,Be^9)$ is not expected. For O^{18}, however, we have qualitative disagreement, which is surprising in view of the good agreement for $O^{18}(d,Li^6)C^{14}$ in Ref. 7. It is, of course, possible that some of the disagreements are due to the effects of nearby (unknown) compound-nucleus resonances, but we would not draw this conclusion unless the disagreements persist for calculations that use more realistic distorted Li^7 waves.

The ratio of the total experimental cross section σ_{expt} to the DWBA prediction is listed in column 5 of Table I. For properly normalized DWBA calculations this ratio $\sigma_{\text{expt}}/\sigma_{\text{DWBA}}$ should be equal to the "cluster" spectroscopic factor S_{x_B} for the target nucleus. It should be mentioned again that the absolute normalization of our DWBA calculations is certain to only about an order of magnitude, so in general there remains a normalization correction factor η which is the *same* for all (d,Li^7) calculations. Once we assume that our model is adequate, the ratio $\sigma_{\text{expt}}/\sigma_{\text{DWBA}}$ for reactions of the same type is a relative measure of the cluster probability in various target nuclei, since the factor a_0^2 is identical for reactions of the same type and need not be known. However, any direct comparison of the ratios for $\sigma_{\text{expt}}/\sigma_{\text{DWBA}}$ between reactions of different types [i.e., (d,Li^6) and (d,Li^7)] will depend upon the product of the factors S_{x_B} and a_0^2. Eventually such spectroscopic ratios should provide details about many-particle correlations in these nuclei. For example, if (d,Li^6) and (d,Li^7) reactions are correctly described as a simple transfer of an alpha and He^5 cluster, respectively, then evidence for the existence or nonexistence of preformed alpha clusters, or many-particle clusters in general, should follow from the magnitude of extracted spectroscopic ratios.

A priori, one might expect (d,Li^7) reactions to have smaller cross sections than (d,Li^6) reactions from corresponding targets if a direct cluster transfer is a realistic picture. Not only should the probability be greater for picking up four particles than five particles, but it also has been argued that the existence of four-particle quasi-alpha clusters is enhanced over other large cluster substructures in nuclei. Furthermore, while most evidence (see footnotes 2, 26, 27, and 28 in Ref. 7) supports a strong $d+\alpha$ parentage in Li^6, similar evidence[9,10] for a strong $d+He^5$ parentage in Li^7 does not exist. In the absence of any detailed spectroscopic calculations, we feel that it is fair to assume that Li^7 looks less like $d+x$ than Li^6. With this qualification, we conclude from Table I that only for the C^{13} target is the ratio $\sigma_{\text{expt}}/\sigma_{\text{DWBA}}$ for (d,Li^6) obviously larger than that for (d,Li^7) or (d,Li^{7*}) reactions. For the other targets, all (d,Li^6) and (d,Li^7) ratios are of comparable magnitude, so that we seem to find a surprisingly large enhancement for all five-nucleon transfers.

F. SUMMARY AND CONCLUSIONS

The experimental (d,Li^7), (d,Be^7), and (d,Be^9) reaction cross sections have absolute magnitudes and angular distributions which are not very different from (d,Li^6) reactions from corresponding targets. This may mean that all these reactions proceed by essentially the same reaction mechanism. In the simple cluster transfer picture, five nucleons may be transferred as $J^\pi=\frac{3}{2}^-$ or $\frac{1}{2}^-$ clusters, and the angular distributions of these many-nucleon transfer reactions normally contain contributions from two possible l transfers. DWBA predictions for (d,Li^7) and (d,Be^7) reactions exhibit roughly the same features as the data, but generally do not show detailed agreement even when sums of two l transfers are considered. All the deficiencies of the (d,Li^6) DWBA calculations discussed in Sec. B of Ref. 7 also exist for the many-nucleon transfer predictions presented here. Still, the predicted cross sections appear to be in fair agreement with the experimental cross sections.

No theoretical attempts were made to assess the overlaps for He^5 clusters in C^{13}, O^{17}, O^{18}, and F^{19}, or for Li^5 and Li^7 clusters in F^{19}. However, for targets in the $2s$, $1d$ shell the $\sigma_{\text{expt}}/\sigma_{\text{DWBA}}$ ratios for (d,Li^7), which should be proportional to the "cluster spectroscopic factors," are of the same order of magnitude as the $\sigma_{\text{expt}}/\sigma_{\text{DWBA}}$ ratios for (d,Li^6) reactions. Since the factor a_0^2 for Li^7 and Be^7 is certainly less than one and may well be close to 0.4 (as assumed), we have a surprisingly large enhancement for all five-nucleon transfers. In conclusion, it is felt that the spectroscopic information suggested by our (d,Li^6) and (d,Li^7) analyses lends no support to assumptions of predominant 4-particle or alpha-clustering in the s-d shell.

ACKNOWLEDGMENTS

The authors are indebted to Dr. R. Drisko who generously provided help in the initial phase of the DWBA analysis, and permitted the continued use of his DWBA computer program JULIE.

The calculations reported in this article were perperformed at the University of Pittsburgh Computation Center, which is partially supported by the National Science Foundation under Grant No. G-11309.

[9] C. Ruhla, M. Riov, J. P. Garron, J. C. Jacmart, and L. Massonet, Phys. Letters **2**, 44 (1962).

[10] C. G. Morrison, N. H. Gale, M. Hussain, and C. Murray, in *Proceedings of the Third Conference on Reactions between Complex Nuclei, Asilomar, 1963*, edited by A. Ghiorso, R. M. Diamond, and H. E. Conzett (University of California Press, Berkeley, California 1963), p. 168.